

Fatigue analysis of deepwater hybrid mooring line under corrosion effect

Dongsheng Qiao^a, Ph. D

Jun Yan^b, M. Sc.

Jinping Ou^{a,b}, Ph. D

a) Deepwater Engineering Research Center, Dalian University of Technology, Dalian, China

b) State Key Laboratory of Coastal and Offshore Engineering, Dalian University of Technology, Dalian, China

ABSTRACT

In the deepwater exploitation of oil and gas, replacing the polyester rope by a wire in the chain-wire-chain mooring line is proved to be fairly economic, but this may provoke some corresponding problems. The aim of this paper is to compare the fatigue damage of two mooring system types, taking into account corrosion effects. Using a semi-submersible platform as the research object, two types of mooring systems of the similar static restoring stiffness were employed. The mooring lines had the chain-wire-chain and chain-polyester-chain structure, respectively. Firstly, the numerical simulation model between the semi-submersible platform and its mooring system was built. The time series of mooring line tension generated by each short-term sea state of South China Sea S4 area were calculated. Secondly, the rain flow counting method was employed to obtain the fatigue load spectrum. Thirdly, the Miner linear cumulative law model was used to compare the fatigue damage of the two mooring system types in long-term sea state. Finally, the corrosion effects from zero to twenty years were considered, and the comparison between the fatigue damage of the two mooring system types was recalculated.

Keywords: Mooring system; short-term sea state; fatigue damage; corrosion effect

INTRODUCTION

Floating platforms and their mooring systems need to resist various ocean environmental conditions. Changes in wind, current, and wave loads provoke variable motion and stress in the mooring system. Gradual accumulation of the variable stress can lead to cumulative fatigue damage. In recent years, many fatigue damages of the mooring line in the practical projects have been recorded [1]. Therefore the investigation of fatigue damage is still necessary, and the problem is discussed by many scholars.

A traditional catenary mooring system is still widely used in practical projects nowadays [2-3]. It usually has the chain-wire-chain structure. With increasing water depth, the weight of the chain and the wire become very large, and the cost becomes uneconomic. Recently, the results of successful development of synthetic fibres have been applied to deepwater mooring system, for instance in the form of the polyester mooring system to FPSO-2 project conducted by Brazil Petroleum Company [4]. Some problems concerning the use of a new type of mooring system can be named, including the fatigue problem discussed in this paper.

At present, the commonly used calculation method of fatigue damage is the Miner linear cumulative law model which is based on the S-N curve, and this method is suggested by many criterions [5-7]. Another calculation method is the

fracture mechanics approach, which is not very mature and still needs to develop [8-9]. That is why the S-N curve was used to calculate the fatigue damage in this paper.

Mathisen et al. [10] applied the S-N curve to calculate the fatigue damage of the mooring system in the DEEPMOOR project, and indicated that the wave responses could provoke more fatigue damage than the drift responses. Omar et al. [11] applied the Dirlik method, the rain flow counting method, the narrowband spectra analysis method, and the broadband spectra revised method to count the mooring line tension, and used the S-N curve to calculate the fatigue damage. Gao and Moan [12] investigated a catenary mooring system for a semi-submersible platform, and calculated the fatigue damage under wave loads and drift loads. Han et al. [13] investigated the influences of different mooring layouts to the fatigue damage of a mooring line. Qiao and Ou [14] calculated the fatigue damage of the polyester mooring line based on the S-N curve. Huang et al. [15] used the Ariane software to calculate the fatigue damage of a taut mooring system in the South China Sea.

The influence of corrosion effects to the fatigue damage is a separate problem. Gao et al. [16] introduced the reliability calculation to the corrosion fatigue damage analysis. Lardier et al. [17] applied the S-N curve and the fracture mechanics method to calculate the fatigue reliability of catenary mooring lines under corrosion effect.

In those research activities, the scholars mainly applied the S-N curve to calculate the fatigue damage of a certain mooring system. This paper aims at comparing the fatigue damage between the chain-wire-chain and chain-polyester-chain mooring systems, taking into account the corrosion effects.

A semi-submersible platform was selected as the research object, along with two mooring system types of similar static restoring stiffness. The Miner linear cumulative law model was used to compare the fatigue damage, and the corrosion effects from zero to twenty years were considered in the calculation.

FATIGUE ANALYSIS THE S-N CURVE

According to American Petroleum Institute (API) Recommended Practice 2SK [6], the S-N curve presents the number of cycles to failure for a specific mooring component as a function of a constant normalized tension range, based on the results of experiments. For mooring systems, the $T - K$ approach which only considers the tension fatigue and ignores the bending fatigue is normally used. The formula (1) presents the $T - K$ curve.

$$NR^M = K \quad (1)$$

where N is the number of cycles, R is the ratio of tension range to reference breaking strength, and M and K are material parameters in the $T - K$ curve.

According to Miner's linear cumulative damage rule, the annual cumulative fatigue damage D can be summed up from the fatigue damage D_i arising in a set of short-term sea states.

$$D = \sum_{i=1}^n D_i \quad (2)$$

The fatigue damage D_i in the i -th short-term sea state:

$$D_i = \frac{n_i}{K} E[R_i^M] \quad (3)$$

where n_i is the number of tension cycles encountered in this short-term sea state, R_i is the ratio of the tension range to the referential breaking strength, $E[R_i^M]$ is the expected value of the normalized tension range R_i raised to the power M .

In the calculations, the values of $M = 9.0$ and $K = 316$ for chain, and $M = 5.05$ and $K = 10^{(3.25 - 3.42 L_m)}$ for wire, were chosen from the $T - N$ curve of wire recommended by API RECOMMENDED PRACTICE 2SK [6]. L_m is the ratio of the mean load to the referential breaking strength for wire. $M = 9.0$ and $K = 7.5$ and were chosen from the curve of polyester recommended by API RECOMMENDED PRACTICE 2SM [18].

CORROSION EFFECT

The corrosion effect has many influence parameters, such as salinity, humidity, current velocity, water depth, etc. Melchers et al. [19] investigated the corrosion on fully submerged chains, and indicated that the mean value of the corrosion rate is slightly smaller than that given in DNV OS-E301 [7]. So, the corrosion rate of the chain used in this paper was

assumed according to the DNV OS-E301. Besides, in practical applications a galvanized or plastic jacket is usually added to the wire or the polyester mooring component to protect against the corrosion effect [6], so only the corrosion effect of the chain was taken into account in this paper.

According to DNV OS-E301, the corrosion rate of a chain is divided into three parts. The corrosion rate in the splash zone is 0.8 mm/year, while the corrosion rates in the catenary and bottom zones are both 0.2 mm/year.

The influence of the corrosion effect to the fatigue damage is mainly represented in two ways. Firstly, the material parameters and in the curve are changed. Secondly, the stress in the mooring line is changed due to the reduction of the chain diameter provoked by the corrosion.

SEMI-SUBMERSIBLE PLATFORM MODEL AND ENVIRONMENTAL CONDITIONS

SEMI-SUBMERSIBLE PLATFORM

The main structure of the semi-submersible platform model consisted of two pontoons, four columns, a deck, and a derrick. The main characteristic parameters are listed in Table 1.

Tab. 1. Parameters of semi-submersible platform

Parameters	Value
Deck (m)	74.42×74.42×8.60
Column (m)	17.385×17.385×21.46
Pontoon (m)	114.07×20.12×8.54
Tonnage (kg)	48206800
Centre of gravity from water surface (m)	8.9
Roll gyration radius (m)	32.4
Pitch gyration radius (m)	32.1
Yaw gyration radius (m)	34.4
Initial air gap (m)	14
Diameter of brace (m)	1.8

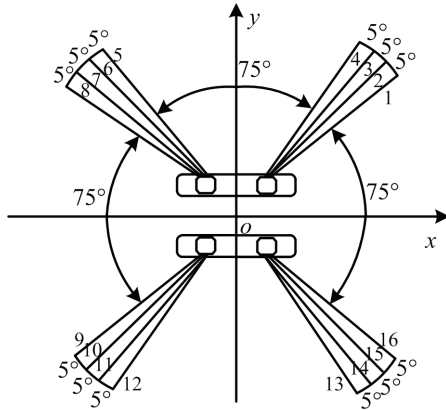


Fig. 1. Mooring system layout

MOORING SYSTEM

The mooring system consisted of four (4x4) groups, as shown in Figure 1. Two mooring system types, which are chain-wire-chain and chain-polyester-chain, were used respectively during the calculation in combination with the semi-submersible platform. The mooring line properties are listed in Table 2. The static characteristics of the two mooring types are compared in Fig. 2 ÷ 3. A representative mooring line was chosen to compare the fatigue damage between the two mooring system types, shown as Fig. 4. According to Handbook of Offshore Engineering [20], the drift stiffness of polyester was used to calculate the fatigue damage.

Item		Steel mooring	Polyester mooring
Water depth (m)		1500	1500
Initial top pretension (KN)		2050	2150
Property of material	upper	K4 Studless Chain	K4 Studless Chain
	middle	Spiral Strand Wire	Polyester
	bottom	K4 Studless Chain	K4 Studless Chain
Line weight in water (N/m)	upper	1431.018	1431.018
	middle	268.036	40.082
	bottom	1431.018	1431.018
Line axial stiffness EA (MN)	upper	603.53	603.53
	middle	626.77	183.81/239.75
	bottom	603.53	603.53
Total line length (m)	upper	450	450
	middle	2000	2000
	bottom	1500	1500
Nominal diameter (mm)	upper	90.0	90.0
	middle	82.55	160.0
	bottom	90.0	90.0
Breaking strength (KN)	upper	8160	8160
	middle	5920	7840
	bottom	8160	8160

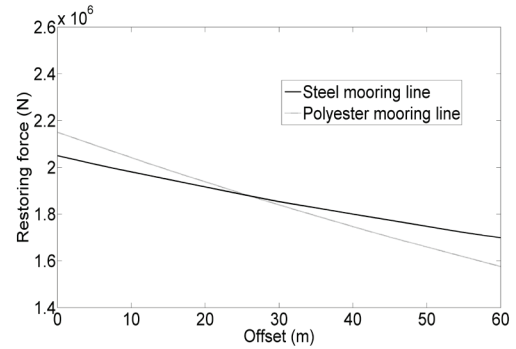


Fig. 2. Comparison of static stiffness of single hybrid mooring line

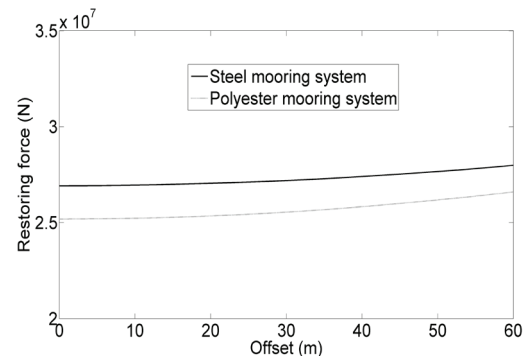


Fig. 3. Comparison of static stiffness of mooring system

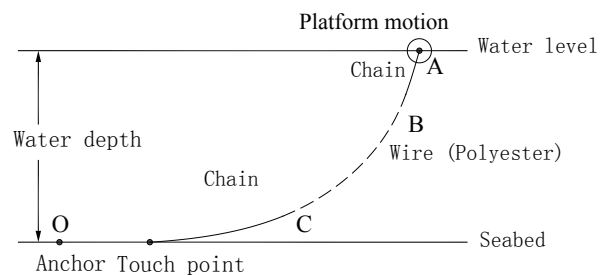


Fig. 4. Mooring line configuration

According to Fig. 2 ÷ 3, the static characteristics of the two mooring system types are similar. Then the two mooring system types were added to the semi-submersible platform.

ENVIRONMENTAL CONDITIONS

Motion responses of the semi-submersible platform were calculated under the combination of wind, current, and wave loads. The sea state condition was selected from the South China Sea S4 area, along with the angle of incidence with respect to the X-axis. The long-term sea state usually consists of a number of short-term sea states. According to the wave scatter diagram of South China Sea S4 [15] in one year, the chosen sea states are listed in Table 3 and the JONSWAP spectra with the peak value $\gamma = 2.0$ were used. H_s is the significant wave height, T_s is the zero up-crossing period. V_s is the wind speed. In the calculations the API wind spectrum was used. \bar{u} is the mean current speed. „p” is the occurrence probability of each sea state.

Tab. 3. Parameter of short-term sea state

Sea state	(m)	(s)	(m/s)	(m/s)	(%)	Sea state	(m)	(s)	(m/s)	(m/s)	(%)
1	0.250	3.5	3.40	0.102	0.1	33	1.050	8	8.40	0.252	1.3
2	0.250	4	3.80	0.114	1.0	34	1.550	8	10.0	0.300	2.5
3	0.675	4	5.60	0.168	0.8	35	2.175	8	12.0	0.360	3.0
4	1.050	4	7.00	0.210	0.7	36	2.875	8	12.8	0.384	3.1
5	1.550	4	8.50	0.255	0.5	37	3.625	8	14.0	0.420	2.2
6	2.175	4	10.1	0.303	0.2	38	4.500	8	15.4	0.462	1.7
7	0.250	5	4.20	0.126	2.9	39	5.500	8	16.5	0.495	0.6
8	0.675	5	6.00	0.180	3.1	40	6.750	8	18.2	0.520	0.2
9	1.050	5	7.60	0.228	3.4	41	0.250	9	5.00	0.150	0.1
10	1.550	5	9.00	0.270	3.7	42	0.675	9	7.00	0.210	0.2
11	2.175	5	10.8	0.324	1.9	43	1.050	9	8.60	0.258	0.4
12	2.875	5	11.6	0.348	0.7	44	1.550	9	10.6	0.318	0.8
13	3.625	5	13.0	0.390	0.1	45	2.175	9	12.6	0.378	1.0
14	0.250	6	4.30	0.129	2.9	46	2.875	9	13.2	0.396	1.2
15	0.675	6	6.40	0.192	3.7	47	3.625	9	14.8	0.444	1.0
16	1.050	6	7.80	0.234	5.0	48	4.500	9	16.0	0.480	1.0
17	1.550	6	9.40	0.282	7.2	49	5.500	9	16.8	0.504	0.6
18	2.175	6	11.2	0.336	5.5	50	6.750	9	18.0	0.540	0.4
19	2.875	6	12.0	0.360	3.2	51	0.675	10	7.50	0.225	0.1
20	3.625	6	13.2	0.396	1.1	52	1.050	10	9.20	0.276	0.1
21	4.500	6	14.5	0.435	0.2	53	1.550	10	12.0	0.360	0.2
22	0.250	7	4.50	0.135	1.5	54	2.175	10	13.4	0.402	0.2
23	0.675	7	6.60	0.198	2.1	55	2.875	10	14.0	0.420	0.3
24	1.050	7	8.20	0.246	3.3	56	3.625	10	15.6	0.468	0.3
25	1.550	7	9.80	0.294	5.7	57	4.500	10	16.7	0.501	0.3
26	2.175	7	11.6	0.348	5.7	58	5.500	10	17.4	0.522	0.2
27	2.875	7	12.4	0.372	4.6	59	6.750	10	19.1	0.573	0.3
28	3.625	7	13.7	0.411	2.4	60	2.875	11	15.2	0.456	0.1
29	4.500	7	15.0	0.450	1.3	61	3.625	11	16.4	0.492	0.1
30	5.500	7	16.1	0.483	0.3	62	4.500	11	17.2	0.516	0.1
31	0.250	8	4.80	0.144	0.5	63	5.500	11	18.0	0.540	0.2
32	0.675	8	6.80	0.204	0.8	64	3.625	12	20.0	0.600	0.1

NUMERICAL SIMULATION

COUPLED MODEL BETWEEN THE SEMI-SUBMERSIBLE PLATFORM AND ITS MOORING SYSTEM

To calculate the coupled motion, the Cummins's method [21] was applied in this study. The wave forces on the semi-submersible platform were calculated using the boundary element method based on the diffraction theory and the commercially available program AQWA [22]. The panel model is shown in Figure 5. The model for the coupled analysis of the semi-submersible platform and its mooring lines is shown in Figure 6. A coupled model of the semi-submersible platform and its mooring system is known from the literature [23]. It was also established by the authors of this paper.

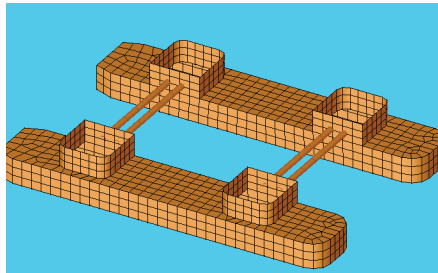


Fig. 5. Panel model

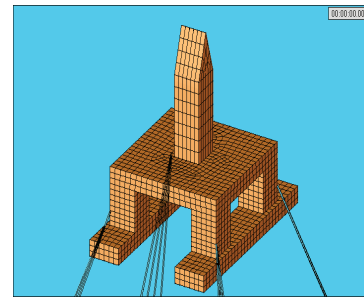
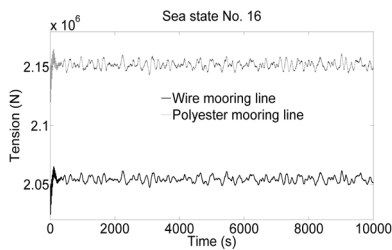
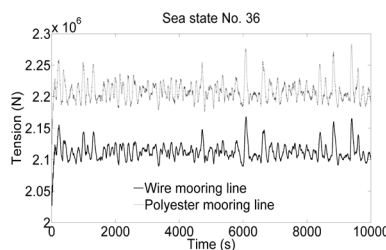


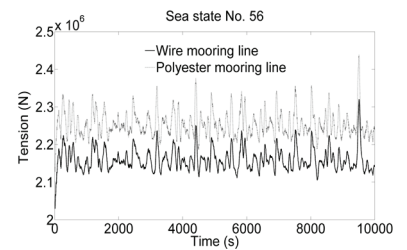
Fig. 6. Coupled analysis model



7(a) sea state No. 16

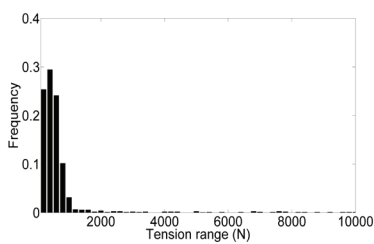


7(b) sea state No. 16

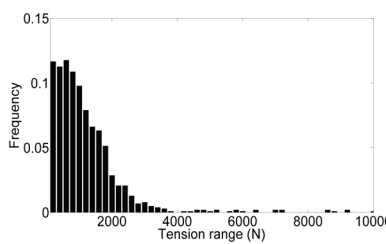


7(c) sea state No. 16

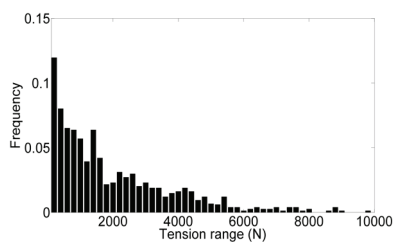
Fig. 7. Time series of mooring line tension at point A without corrosion



8(a) sea state No. 16

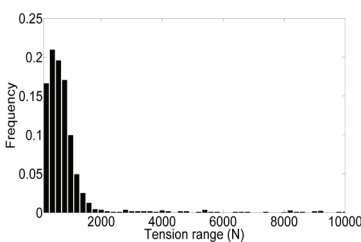


8(b) sea state No. 36

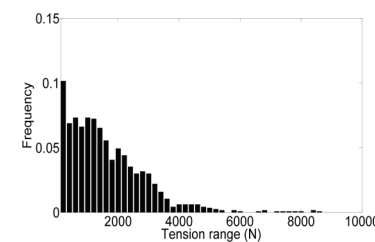


8(c) sea state No. 56

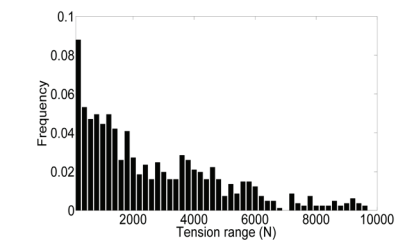
Fig. 8. Fatigue load spectra of point A in steel mooring line without corrosion



9(a) sea state No. 16



9(b) sea state No. 36



9(c) sea state No. 56

Fig. 9. Fatigue load spectra of point A in polyester mooring line without corrosion

FATIGUE LOAD SPECTRA

In the comparative analysis of fatigue damage, the fatigue load spectra of the mooring line need to be obtained firstly. In this study, the rain float counting method [24] was employed to count the mooring line tension. A histogram of the tension range can be obtained from this counting, in the form of fatigue load spectra of the mooring line.

A time series of the mooring line tension at point A (shown in Fig. 4) between the two mooring system types under sea states No. 16, 36, 56 are plotted in Figure 7, and the corresponding fatigue load spectra are plotted in Figures 8 ÷ 9. The results under other sea states are omitted for brief.

The statistic analysis of the fatigue load spectra in all short-term sea states reveals that they don't satisfy the normal theory probability distribution. Therefore the histograms were employed to reflect the short-term distribution of tension range under all short-term sea states, and the rain flow counting results were used to calculate the fatigue damage directly in the later study.

FATIGUE ANALYSIS

Based on the abovementioned fatigue damage calculation method, the fatigue damages of the two mooring system types were calculated. The fatigue damages of Point A, B, and C, which represent the upper end point of three segments in the mooring line (shown in Fig. 4), were compared without the corrosion effect. Then, the corrosion effect after 5 years, 10 years, 15 years, and 20 years was taken into account. The fatigue damages of Point A, B, and C under each short-term sea state were recalculated under the effect of the corrosion rate.

FATIGUE DAMAGE WITHOUT CORROSION

The fatigue damages of the two mooring system types under each short-term sea state are plotted in Fig. 10 ÷ 11, and the comparisons of point A, B, and C are plotted in Fig. 12 ÷ 14. The vertical-axis is the logarithm of fatigue damage. According to Fig. 10 ÷ 11, in both cases of the two examined mooring system types the main fatigue damage occurred in the chain segment, independently of the fact whether the mooring line has the chain-wire-chain or the chain-polyester-chain structure. At the same time, the fatigue damage in the wire or polyester segment is relatively much smaller. In the chain-wire-chain mooring line, the fatigue damage in the upper chain is obvious larger than in the bottom chain, while for the chain-polyester-chain mooring line the fatigue damage in the upper chain is almost the same as in the bottom chain. This phenomenon should need additional attention in the practical project. When using the chain-polyester-chain mooring system, the most possible fatigue damage zone includes not only the upper chain in the splash zone, but also the bottom chain.

According to Fig. 12 ÷ 14, the fatigue damage of point B in the steel mooring line is larger than the one in the polyester mooring line, but the fatigue damages of point A and C in the steel mooring line are smaller than those in the polyester mooring line. In other words, replacement of the polyester rope for the wire in the chain-wire-chain mooring line resulted in a much smaller fatigue damage than that observed for the wire, but also provoked fatigue damages of the upper and bottom chains which are larger than those recorded for the chain-wire-chain mooring line. This interesting phenomenon still needs additional attention in the practical project. The replacement of the polyester rope for the wire in the chain-wire-chain mooring line means immolating the fatigue life of the chain to improve the fatigue life of middle segment.

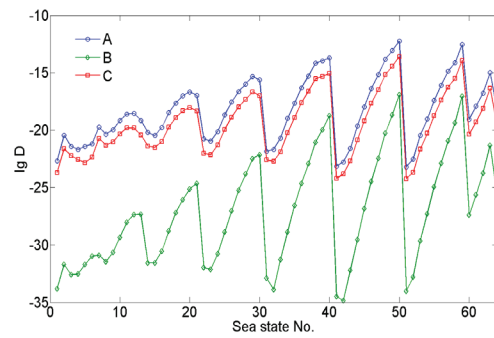


Fig. 10. Fatigue damage of steel mooring lines under short-term sea states without corrosion

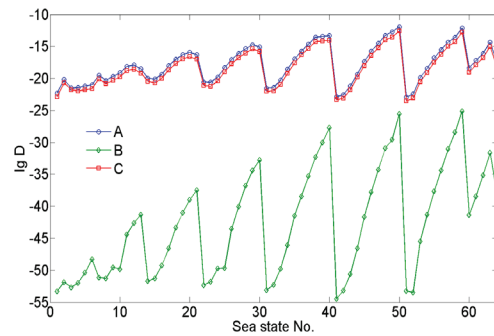


Fig. 11. Fatigue damage of polyester mooring lines under short-term sea states without corrosion

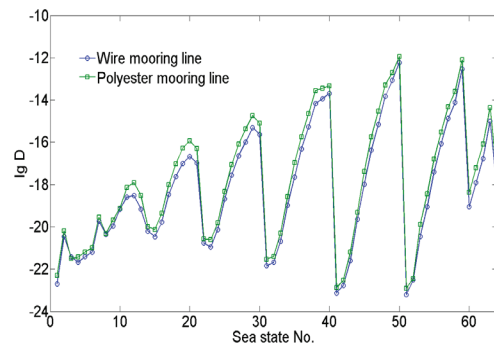


Fig. 12. Fatigue damage of point A under short-term sea states without corrosion

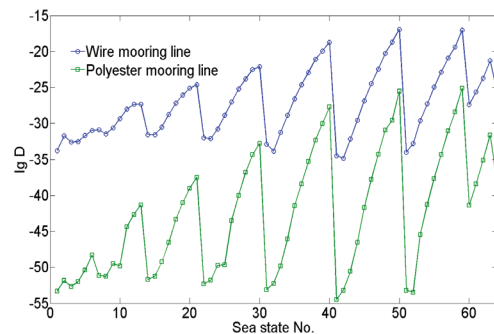


Fig. 13. Fatigue damage of point B under short-term sea states without corrosion

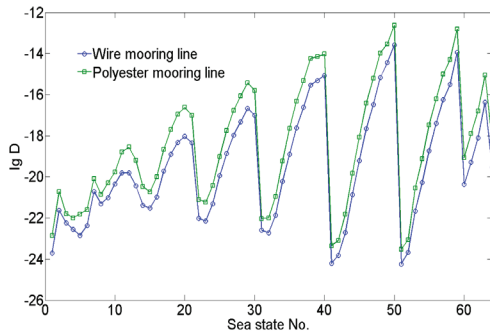


Fig. 14. Fatigue damage of point C under short-term sea states without corrosion

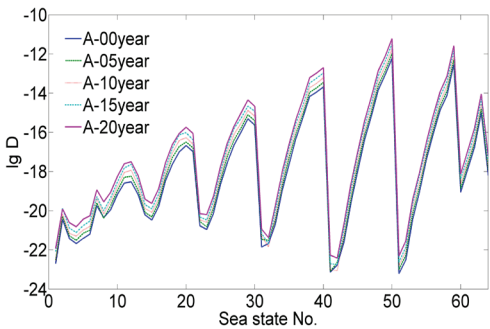


Fig. 15. Fatigue damage of point A in steel mooring lines under short-term sea states with corrosion

FATIGUE DAMAGE WITH CORROSION IN DIFFERENT YEARS

Results of analysing the corrosion effect in different years are shown in Fig. 15 as the fatigue damages of point A in the steel mooring line under each short-term sea state, and in Fig. 16 ÷ 20 as the fatigue damages of two mooring system types under different years.

According to Fig. 15 ÷ 17, the nature of changes of fatigue damage under corrosion is similar to that without corrosion. With the increasing corrosion years, the fatigue damage increases under each short-term sea state. Meanwhile, the increase of the fatigue damage of point A under long-term sea state is much larger than the one of point B and C. This phenomenon indicates that the upper chain in the splash zone needs additional attention with respect corrosion effects.

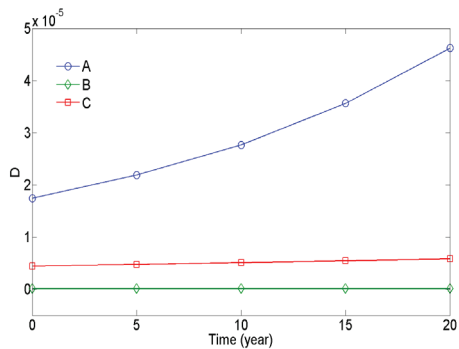


Fig. 16. Fatigue damage of steel mooring lines with corrosion

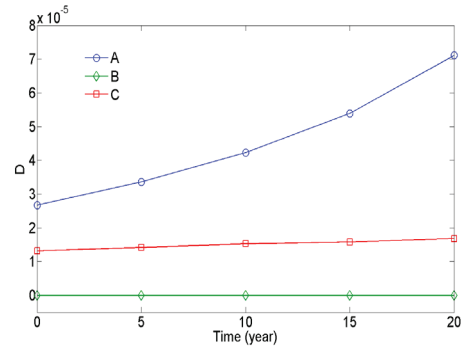


Fig. 17. Fatigue damage of polyester mooring lines with corrosion

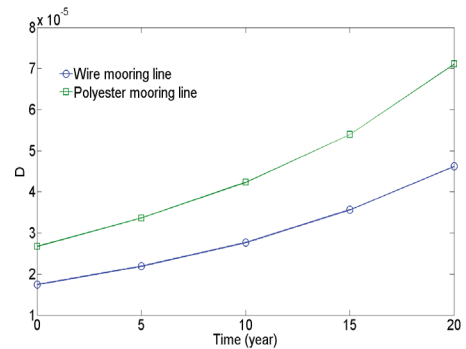


Fig. 18. Fatigue damage of point A with corrosion

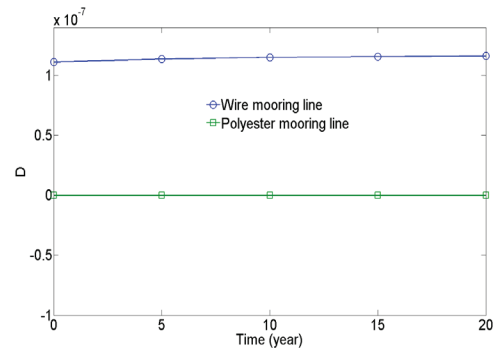


Fig. 19. Fatigue damage of point B with corrosion

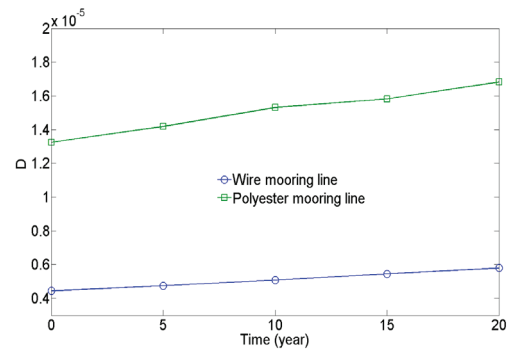


Fig. 20. Fatigue damage of point C with corrosion

According to Fig. 18 ÷ 20, the difference in the scale of the fatigue damage between the two mooring system types is getting bigger with the increasing corrosion years. Under the 20-year corrosion effect, the difference between the fatigue damage of the two mooring system types at point A, B, and C is much larger than the ones without corrosion. In other words, the corrosion effect increases the difference between the fatigue damages of the two mooring system types.

CONCLUSIONS

The fatigue damages between the chain-wire-chain and chain-polyester-chain mooring systems applied for a semi-submersible platform were compared. The two types of mooring systems had a similar static restoring stiffness. The analysis took into account the corrosion effect. The following preliminary findings can be formulated:

- The fatigue load spectra of the mooring line don't satisfy the normal theory probability distribution and the rain flow counting results needs to be used directly in calculating the fatigue damage.
- The main fatigue damage occurred in the chain segment, and the fatigue damage in the wire or polyester segment is relative much small. In the chain-wire-chain mooring line, the fatigue damage in the upper chain is obvious larger than in the bottom chain, while in the chain-polyester-chain mooring line the fatigue damage in the upper chain is almost the same as in the bottom chain.
- The replacement of polyester rope for the wire in chain-wire-chain mooring line provokes the fatigue damage which is much smaller for the polyester than for the wire, but simultaneously the fatigue damages of the upper and bottom chains in the chain-polyester-chain mooring line are larger than those in the chain-wire-chain mooring line.
- The nature of fatigue damage changes under corrosion effect is similar to that without corrosion. With the increasing corrosion years, the fatigue damage under each short-term sea state also increases.
- Under the corrosion effect, the increase of the fatigue damage of point A under long-term sea state is much larger than the one of point B and C. The corrosion effect increases the difference between the fatigue damage of the two mooring system types.

ACKNOWLEDGEMENTS

This paper is funded in part by National Basic Research Program of China (Grant NO. 2011CB013702; 2011CB013703), National Natural Science Foundation of China (Grant NO. 51209037; 51221961), and China Postdoctoral Science Foundation Funded Project (Grant NO. 2013T60287), and Fundamental Research Funds for the Central Universities (Grant NO. DUT14RC(4)30).

BIBLIOGRAPHY

1. K. T. Ma, A. Duggal, P. Smedley, D. L'Hostis, and H. B. Shu, *A historical review on integrity issues of permanent mooring systems*, in Offshore Technology Conference, Houston, TX, USA, 2013.
2. J. Mohanraj, S. Cawthorne, S. Alverley, S. L. Fletcher, and J. Verwaayen, *Development of a new generation of innovative synthetic wire mooring ropes*, in Offshore Technology Conference Brazil, Rio de Janeiro, Brazil, 2011.
3. J. W. Beck and N. J. Vandeworm, "Mooring system design for a circular hull shape FPSO floater with spar like responses", in Offshore Technology Conference Brazil, Rio de Janeiro, Brazil, 2011.
4. P. Barusco, *Mooring and anchoring systems developed in Marlin Field*, in Offshore Technology Conference, Houston, Texas, 1999.
5. ISO, Petroleum and Natural Gas Industries-Specific Requirements for Offshore Structures-Part 7: Station Keeping Systems for Floating Offshore Structures and Mobile Offshore Units, 2005.
6. American Petroleum Institute-API, Recommended Practice for Design and Analysis of Station Keeping Systems for Floating Structures-API RECOMMENDED PRACTICE 2SK, 2005.
7. Det Norske Veritas-DNV, Offshore Standard-Position Mooring-DNV OS-E301, 2004.
8. J. Mathisen and K. Larsen, *Risk-based inspection planning for mooring chain*, Journal of Offshore Mechanics and Arctic Engineering, vol. 126, no. 3, pp. 250-257, 2004.
9. T. Lassen, J. L. Arana, L. Canada, J. Henriksen, and N. K. Holthe, *Crack growth in high strength chain steel subjected to fatigue loading in a corrosive environment*, in Proceedings of the 24th International Conference on Offshore Mechanics and Arctic Engineering, Halkidiki, Greece, 2005.
10. J. Mathisen, T. Hørte, V. Moe, and W. Lian, *DEEPMOOR-design methods for deep water mooring systems, calibration of a fatigue limit state-DNV Report, No. 98-3110*, 1999.
11. V. A. Omar, E. G. Bruno, and S. L. V. Sudati, *Fatigue analysis and reliability of floating production systems mooring lines in deepwater*, in Proceedings of the 17th International Conference on Ocean, Offshore and Arctic Engineering, Lisbon, Portugal, 1998.
12. Z. Gao and T. Moan, *Wave-induced fatigue damage of mooring chain under combined non-gaussian low and wave frequency loads*, in Proceedings of 25th International Conference on Offshore Mechanics and Arctic Engineering, Hamburg, Germany, 2006.
13. J. S. Han, Y. H. Kim, Y. J. Son, and H. S. Choi, *A comparative study on the fatigue life of mooring systems with different composition*, in 9th International Conference on Hydrodynamics, Shanghai, China, 2010.
14. D. S. Qiao and J. P. Ou, *Calculation on fatigue damage of deepwater catenary hybrid mooring line*, Journal of Ship Mechanics, vol. 16, no. 4, pp. 422-432, 2012.

15. W. Huang, H. X. Liu, G. M. Shan, and C. Hu, *Fatigue analysis of the taut-wire mooring system applied for deep waters*, China Ocean Engineering, vol. 25, no. 3, pp. 413–426, 2011.
16. Z. Gao, T. Moan, and S. E. Heggelund, *Time variant reliability of mooring system considering corrosion deterioration*, in Proceedings of the 24th International Conference on Offshore Mechanics and Arctic Engineering, Halkidiki, Greece, 2005.
17. J. Lardier, T. Moan, and Z. Gao, *Fatigue reliability of catenary mooring lines under corrosion effect*, in Proceedings of the 27th International Conference on Offshore Mechanics and Arctic Engineering, Estoril, Portugal, 2008.
18. American Petroleum Institute–API, Recommended Practice for Design, Manufacture, Installation, and Maintenance of Synthetic Fiber Ropes for Offshore Mooring Upstream Segment–API RECOMMENDED PRACTICE 2SM, 2001.
19. R. E. Melchers, T. Moan, and Z. Gao, *Corrosion of working chains continuously immersed in seawater*, Journal of Marine Science and Technology, vol. 12, no. 2, pp. 102–110, 2007.
20. S. K. Chakrabarti, Handbook of Offshore Engineering, Elsevier, the Boulevard, Langford Lane, Kidlington, Oxford OX5 1GB, UK, 2005.
21. W. E. Cummins, The Impulse Response Function and Ship Motions, Washington DC, DTMB, Report No. 1661, 1962.
22. AQWA User Manual, AQWA-LINE Manual, Horsham, Century Dynamics Limited, 2006.
23. D. S. Qiao and J. P. Ou, *Global responses analysis of a semi-submersible platform with different mooring models in South China Sea*, Ships and Offshore Structures, vol. 8, no. 5, pp. 441–456, 2013.
24. N. E. Dowling, *Fatigue failure predictions for complicated stress-strain histories*, Journal of Materials, vol. 7, no. 1, pp. 71–87, 1972.

CONTACT WITH THE AUTOR

Dongsheng Qiao, Ph. D

Faculty of Infrastructure Engineering,
Building 4#, Room 306,
Dalian University of Technology,
Linggong Road No.2, Dalian, Liaoning,
116024, China

Telephone: 8641184706742

Fax: 8641184706652

Email: qds903@163.com